LAPPEENRANTA UNIVERSITY OF TECHNOLOGY
School of Technology
Technical Physics

Grigoryeva Maria

REDUCING CONTACT RESISTANCE IN GRAPHENE DEVICES

Examiner: Professor Erkki Lähderanta
Professor Harri Lipsanen
Thesis instructor: D. Sc. Juha Riikonen

Abstract

LAPPEENRANTA UNIVERSITY OF TECHNOLOGY

School of Technology

Technical Physics

Grigoryeva Maria

Reducing contact resistance in graphene devices

Master's thesis

4.6.2014

39 pages, 21 figures and 1 table
Examiner: Professor Erkki Lähderanta
Professor Harri Lipsanen
Thesis instructor: D. Sc. Juha Riikonen
Keywords: graphene, contact resistance, metal-graphene junction, Ni contacts, GFET

In this thesis, the contact resistance of graphene devices was investigated because high contact resistance is detrimental to the performance of graphene field-effect transistors (GFET). Method for increasing so-called edge-contact area was applied in device fabrication process, as few nanometers thick Ni layer was used as a catalytic etchant during the annealing process. Finally, Ni was also used as a metal for contact. GFETs were fabricated using electron beam lithography using graphene fabricated by chemical vapor deposition (CVD).

Critical part of the fabrication process was to preserve the high quality of the graphene channel while etching the graphene at contact areas with Ni during the annealing. This was achieved by optimizing the combination of temperature and gas flows. The structural properties of graphene were studied using scanning electron microscopy, scanning confocal μ-Raman spectroscopy and optical microscopy. Evaluation of electric transport properties including contact resistance was carried out by transmission line method and four-probe method. The lowest contact resistance found was about at 350 Ωμm.

In addition, different methods to transfer CVD graphene synthesized on copper were studied. Typical method using PMMA as a supporting layer leaves some residues after its removal, thus effecting on the performance of a graphene devices. In a metal assisted transfer method, metal is used as an interfacial layer between PMMA and graphene. This allows more effective removal of PMMA. However, Raman spectra of graphene transferred by metal assisted method showed somewhat lower quality than the PMMA assisted method

Acknowledgements

I want to thank my supervisors Prof. Harri Lipsanen and Prof. Erkki Lahderanta for the opportunity to do my master thesis in the Nanotechnology research group at the Department of Micro and Nanoscience in Aalto University. I also want to extend my special thanks to my thesis advisor D.Sc. Juha Riikonen for ideas, discussions and without whom this work simply would not take a place. I wish also to thank Wonjae Kim, Changfeng Li, Susoma Jannatul, Olli Svensk and Lauri Riuttanen for patient guidance and giving very useful instructions during my work. Finally, I want to thank my family and friends for supporting me despite of borders and distances between us.

Espoo, 04.06.2014

Maria Grigoryeva

Abbreviations

APS	Ammonium persulphate
AFM	Atomic force microscopy
CVD	Chemical vapor deposition
FLG	Few-layer graphene
GFET	Graphene field-effect transistor
QHE	Quantum Hall effect
OPVs	Organic photovoltaics
PL	Photoluminescence
PMMA	Polymethyl-methacrylate
SLG	Single-layer graphene
SEM	Scanning electron microscopy
DI water	deionized water

Symbols

ρ_l	longitudinal resistivity
ρ_h	hall resistivity
μ	carrier mobility
ρ_c	specific contact resistivity
ρ_s	sheet resistivity

Contents

1 Introduction

Nowadays requirements for electronic devices include efficient and fast data processing, small size, and multifunctionality. The development of nanotechnology has provided methods to implement electronic devices with a precision of few nanometers. Detailed investigation of existing materials and their properties led to the discovery of graphene, a new material with attractive properties even for the industry. Graphene is a real breakthrough in the material science. Firstly, it has very interesting electronic and mechanical properties, but it also opened the world of 2D materials. Since it was discovered in 2004, investigation of the material itself and ways to exploit it started.

Graphene is an allotrope of carbon, which is physically strong and thermally stable. It has high electron mobility, high thermal conductivity, and long free mean path of carriers; these properties are very useful from application point of view. Other characteristics are scientifically interesting for research, such as quantum Hall effect at a room temperature and spin transport.

Graphene is quite new and promising material, but it needs time to mature. We can see that there are already some examples where graphene has replaced other materials, but application which uses electrical properties is still in the future. Contacts play an important role in the performance of electronic devices. Good metal-graphene junction is required to achieve for example excellent frequency characteristic of devices, hence good power efficiency, low power consumption and small switching times. Achieving a low contact resistance is an actual challenge for all graphene devices at the moment.

The aim of this work was to investigate ways to reduce contact resistance. There are many methods and techniques, and also theoretical and experimental data about suitable metals for graphene, but value of contact resistance still remains high. In this work, graphene obtained by chemical vapor deposition (CVD) was used. Device structures were patterned using EBL and the

metal contacts were deposited with electron beam evaporator. Finally, the devices were characterized with different electrical measurement.

Chapter two of this thesis describes the fundamentals of graphene, and devices, CVD growth, and basics of the contact resistance. Methods of graphene quality confirmation and the electrical measurements are described in chapter three. Chapter four presents the experimental methods used in this study. In chapter five, results are presented and discussed and the summary of the study is in chapter six.

2 Graphene

2.1 Introduction to graphene

In 2004 Andre Geim and Konstantin Novoselov managed to obtain flakes of graphite only few atom layers thick by peeling with ordinary tape. It was first the exfoliated graphene, planar sheet of carbon atoms, densely packed together into a honeycomb shaped crystal lattice (Fig.1). Truly 2D material, which can form different types of other dimensionality carbon structures [1]. Graphene is a 2D building material for carbon materials of all other dimensionalities. It can be wrapped up into 0D fullerenes, rolled into 1D nanotubes or stacked into 3D graphite.

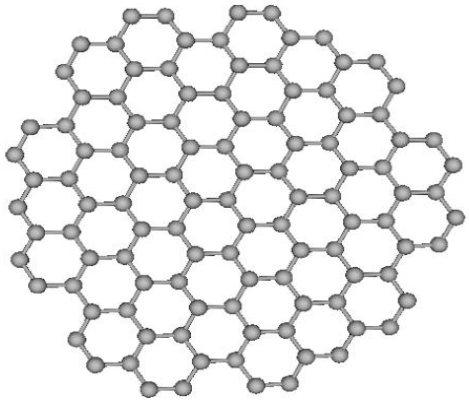

Figure 1. Carbon atoms packed together into a honeycomb crystal forming graphene.

In the first report about graphene, authors claimed that they had observed an electric field effect in a thin carbon films, namely few-layer graphene (FLG). Surprising high value of carrier mobility (μ) ~ 10,000 cm^2/Vs was determined in the new material. Anomalous quantum Hall effect (QHE) was observed even at a room temperature [2]. One of the most interesting aspects of the graphene is its highly unusual behavior of charge carriers as massless relativistic particles (Dirac fermions), this nature of carriers can explain some of quantum effects. Studies of Shubnikov-de Haas (ShdH) oscillations in both longitudinal resistivity ($\boldsymbol{\rho_l}$) and Hall resistivity ($\boldsymbol{\rho_h}$) confirm that electronic

transport in FLG is two dimensional [3]. Graphene has zero band gap as the band structure of a single layer exhibits conductance and valence bands intersecting in two inequivalent points K and K' (Dirac points) in the reciprocal space. Dirac point is defined as a point with minimum conductance, where the charge carriers are tuned between electrons and holes. The Dirac point can be shifted with the gate voltage. Dependence of the sheet resistivity and Hall coefficient on the gate voltage is shown on the Fig.2.

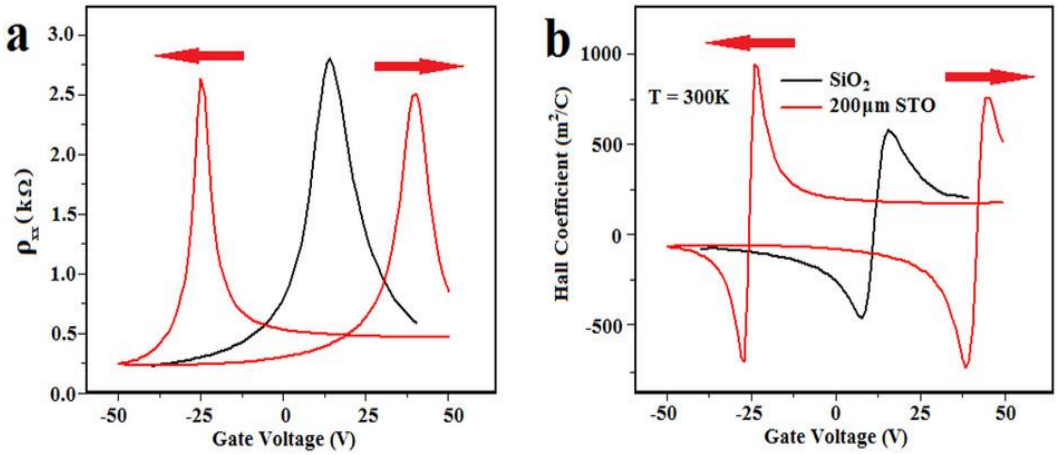

Figure 2. a) Dependence of the sheet resistivity on the back gate voltage and b) dependence of the Hall effect on the back voltage [4].

Absorption of incident light in graphene is about 2.3 % for the wavelengths from 300 to 2500 nm with the peak in 250 nm in UV zone. Also increasing trend in absorption of the light with increasing the number of layers has been observed [5] [3].Physical and thermal properties are also attracting a lot of attention. Mechanically graphene has the highest elastic modulus and strength among others. An intrinsic strain in graphene can influence the electric properties, for example, tensile stress can give information about stress transfer of individual bonds. Devices built on graphene are thermally reliable; graphene has great thermal conductivity in ambient air up to 5000 W/mK whereas supported graphene conductivity is about 500 W/mK [3].

2.2 Chemical vapor deposition of graphene layers

Cost-effective fabrication methods are required to utilize graphene in real-life applications. New synthesis techniques, like a CVD, open up new opportunities for semiconductor the industry. Improving methods to obtain graphene, the characteristics of devices can also be improved, for example graphene field-effect transistors (GFET), graphene sensors and solar cells.

Fabrication of large area graphene sheets with a high quality is an important challenge. First widely used method was graphene exfoliation by repeated peeling [2]. It is a mechanical way to produce small area graphene from natural graphite. Due to the fact that industry requires large area films on different substrates and controllable quality, other methods are considered, such as epitaxial growth in ultrahigh vacuum [4], atmospheric pressure graphitization of SiC [6]. Among all this methods graphite growth by a pyrolysis of hydrocarbons like acetylene and methane has been known since 1960s. CVD is a well-known method, which is used to grow thin films from gaseous sources: gas at a high temperature decomposes into molecules and deposits on the substrate [7]. In case of Cu as a catalytic substrate hydrocarbon decomposition and graphene deposition occur on the surface due to the low solidity of carbon to copper [8].

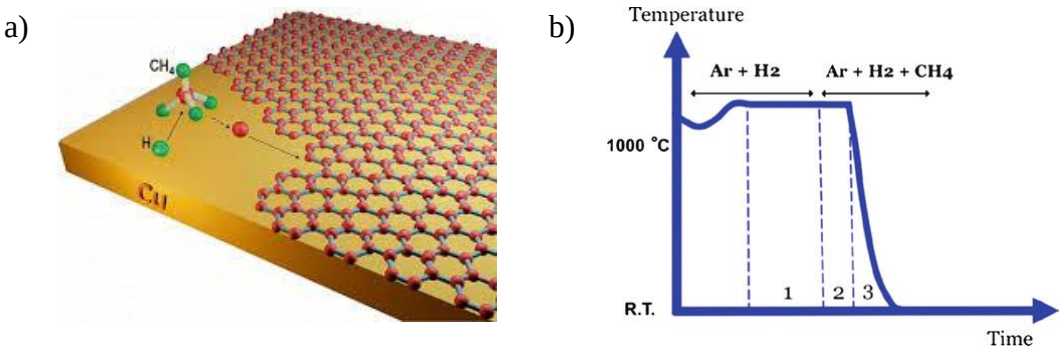

Figure 3. a) Schematic of the graphene growth and b) temperature-time diagram of the graphene growth [9].

Graphene growth consists of several steps; Fig.3a shows simple explanation of the CVD process. Single-layer graphene (SLG) is usually prepared on the Cu foil. Substrate is placed into a reactor; firstly it is annealed in a H_2 ambient to remove any copper oxides from the surface. To grow graphene the chamber is filled by gas mixture of CH_4/H_2. The temperature is usually kept around 950-1000 °C, and finally the sample is cooled down [10].

Temperature-time diagram (Fig.3b) helps to understand the growth process, first part refers to the annealing of the Cu foil, second part of the diagram is the graphene synthesis using methane. On the third part, the reactor is cooled to the room temperature. Dependence of the graphene quality on the growth temperature has been observed in [10]: too low temperature results in disordered carbon the surface or highly defected material. It was found that the optimal temperature is 950 °C. Cooling time is also very important in this process, because ultra-fast cooling can cause a lot of defects and too slow cooling is time consuming [8].

Benefits of the CVD growth are as follows: it is industrially effective and a cost-effective method to obtain enough large-area graphene films. It is reproducible and suitable for industrial scale processing as it is possible to have identic graphene films from the one process to another. Whereas with exfoliation, one can obtain a high purity single-domains, but flakes are randomly

scattered on the substrate. On the other hand, it must be mentioned that in CVD the quality of graphene depends considerably on the quality of the substrate, thus the selection of the catalyst is crucial. Fortunately, copper is not unique material for substrate. Actually Cu is the second generation of catalysts for the graphene grows process, CVD was initially synthesized on the Ni substrates [9]. Moreover, the on-going work for optimizing the CVD growth has already led to significant improvements of graphene uniformity and overall quality. Fabrication of graphene film by CVD was not carried out as a part of this thesis.

2.3 Graphene devices

2.3.1 Graphene based field effect transistor

It has become evident that the exceptional properties of graphene, especially electrical and optical characteristics make it very attractive to the semiconductor industry. High carrier mobility, long electron mean free path and field effect in a 2D material led to big efforts in exploring the fundamental physics and chemistry of graphene. As was mentioned above, graphene has no band gap, thus there is no on/off regime which is required for logic application. Field-effect transistors based on graphene [2] have led to active learning of the material from this side. Two basics types of GFET structures are shown in the Fig.4.

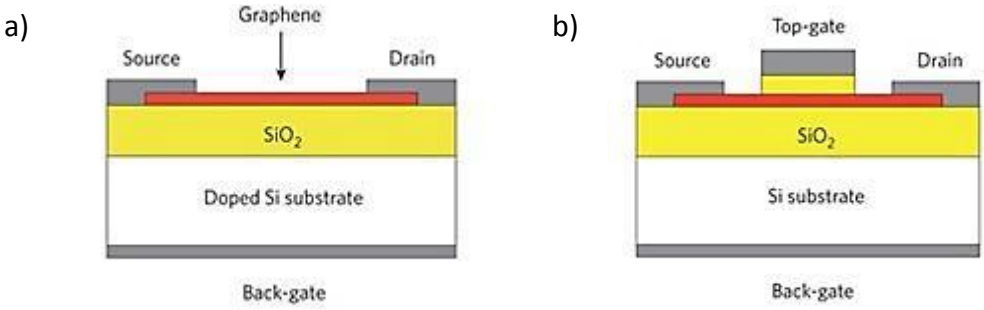

Figure 4. Schematic of a GFET with a) back gate and b) top gate [11].

Ambipolar behavior of a graphene is used to control GFETs by applying back-gate or top-gate voltages. Concentration of charge carriers and their type in the channel is regulated by the potential difference between the channel and the gate. Positive gate voltages provide an electron accumulation in the channel (n-type channel), and negative creates p-type channel. The difference between the work functions of the gate metal and graphene, and any doping of graphene influence on the position of the Dirac point. Nowadays, on/off ratios achieved for GFET are about 100 and 2000 at room temperature and at 20 K, respectively [11].

2.3.2 Other graphene devices

Graphene is highly promising for solar cells and for different sensors in as electrochemical and biological applications. Graphene is very sensitive to a changes in the environment [3]. Three main advantages in applying graphene in gas sensors: in a SLG sheet all atoms can be considered as surface atoms and they are able to adsorb gas molecules, different bonding mechanism between graphene sheets and adsorbates, and electrical properties which lead to a sensitive dependence in the resistance and conductance. Bonding mechanisms change from weak Van der Waals interactions to a strong covalent bonding. Thus, gas detection is mainly based on a graphene conductance changes upon the adsorption of the sensing species. Some of the adsorbates act as dopants changing the charge carrier concentration of graphene. Other kind of gases can cause covalent bonding with graphene [12].

A huge number of polymers and nanoparticle composites are based on the unique properties of graphene. Graphene and its derivatives can be used as fillers for polymer matrix composites, which will also have interesting electrical and thermal properties related to graphene. Derivatives of a graphene are compatible with the polymer matrix and can increase interfacial interaction with the matrix. Thus graphene has great potential for various important applications, for example, structures with high strength and light weight for automobile or

aerospace. On other hand, composites for energy storage, antistatic coatings and electromagnetic interference shielding have already been demonstrated [3].

It was mentioned earlier that graphene was found to absorb a significant (α= 2.3%) fraction of incident white light considering that it is only one monolayer thick. These properties make graphene a promising candidate for practical organic photovoltaics (OPVs). Combining π-conjugated polymers and graphene in solar cells is a possible way to improve efficiency of energy conversion. Industry will have not only size and low cost, but exceptional electronic quality, which is a limiting factor for conjugated polymers [13].

2.4 Contact resistance in metal-graphene junction

Junctions between metal and semiconductor have been known for a long time. Main characterization of the contacts is current-voltage curve, which can have linear or nonlinear dependence. Contacts which demonstrate linear curve are named ohmic, others non-ohmic. Investigation of ohmic contacts started with Schottky's assumption. Then study continued by other outstanding physicist, full review of different types of contacts and mechanisms of current flow is presented in [14].

Concerning metal-graphene junction, first problem we are facing is carrier transport from three dimensional material to two dimensional material, which have quite different densities of states and work functions. The on/off ratios in all transistors are "controlled" by the back gate voltage, because graphene is zero band gap material. The current of graphene is limited by the contact resistance, which is a challenge in the application of graphene for electronic devices. Dependence of the contact resistance on different factors has been investigated [15] [16]. On the one hand, papers report about the variation of the graphene work function under different metals, and that finding the best material for contacts remain an open question. On the other hand, experimental results show that contact resistance does not depend on the metal work function. Nowadays good values of the contact resistance have been achieved by Ni and Pd contacts [15].

Another question is the type of the contacts, distinguishing two main types: edge and top contacts [17]. Edge contacts seem to be more effective and show reduced contact resistance compared with top contacts due to the mechanism of the current flow. Different groups have reported about reduced contact resistance based on the mechanism of the edge-contacted current injection [18] [19]. Several methods have been proposed to increase edge-contact area between graphene and metal, they are patterning during electron beam lithography (EBL) process or by laser [18] [20] and metal-catalyzed etching

[19]. In first two cases the area of edge junction between graphene and metal is increasing by cutting of graphene in the contact area, thus edge-contacted injection is formed. Catalytic properties of transition metals have been known for a long time. Initially, they have been used for graphite etching [21], later for graphene also [22]. In reference [19], the authors formed nanoparticles of Ni on the top of graphene, which etched graphene and showed similar effect of the edge-contacted injection. Suitable temperature and gas flow parameters prevent lateral movement and etching of graphene in crystallographic directions by Ni particles, but provided a localized edge etching of graphene by the catalytic nanoparticles.

3 Characterization of graphene

3.1 Methods of graphene quality confirmation

Performance of graphene devices highly depend on the number of graphene layers and imperfections of the films, thus it is very important to determine quality of graphene on the first steps of device fabrication. Despite that CVD graphene layer should be uniform; we can have bi- or multilayer areas, grains and voids related to the surface irregularities of the CVD substrate. Also transfer of the films can influence on the uniformity. Scanning electron microscopy (SEM), atomic force microscopy (AFM), high resolution optical microscopy and scanning confocal μ-Raman spectroscopy are widely used as characterization techniques of graphene. They are accurate, reliable and fast methods to ensure graphene with high quality before device fabrication.

3.1.1 Optical microscopy

Characterization of a graphene films by an optical microscope is based on Fresnel's law, several papers report about influence of thickness and substrate material, spectrum of light source and thickness of the graphene sheets on total the color deference and the contrast [23] [24]. In this thesis, CVD graphene films on SiO_2/Si substrates with a 285 nm oxide thickness were studied using an optical microscope with white light source. These substrates have been found to give the best contrast for graphene [24]. Optical microscopy was used to detect voids, large wrinkles and other graphene imperfections. This is a rapid way to initially analyze graphene after transfer, before proceeding to more detailed and time consuming methods of characterization.

3.1.2 Scanning Electron Microscopy

Scanning electron microscopy is a straightforward method to characterize graphene film. It gives higher resolution and magnification than optical microscopy. The incident beam is focused by electron lenses and the produced signal is collected and amplified with a detector and photomultiplier respectively.

Different signals can be detected, for example, secondary electrons, back-scattered electrons, characteristic X-rays and cathodoluminescent light. Intensity of the signal is represented as a brightness of the pixel in a digital image. Three typical contrasts can help to characterize graphene; they are surface roughness contrast, edge contrast and thickness contrast.

Several imperfections can be clearly obtain by SEM, related to the different steps of the graphene fabrication. The growth process can form bi- or multilayer flakes, the transfer process can create folds, ruptures, wrinkle or voids. Fig.5 displays typical imperfections, which can be readily observed in the SEM images. It has also been reported that it would be possible to see polymer residues after PMMA has been removed by acetone [25].

a) b)

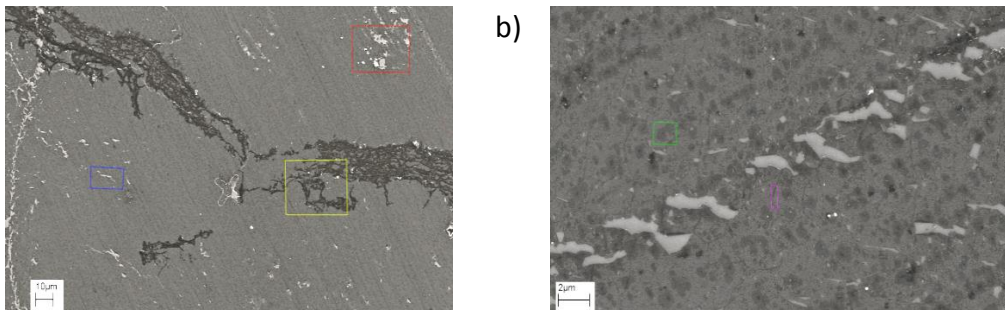

Figure 5. Typical SEM images of graphene sheets a) red box shows voids, blue folds, yellow ruptures and b) green box shows bilayer graphene, pink grains.

3.1.3 Raman spectroscopy

Raman spectroscopy is based on the effect, which was discovered by Chandrasekhar Raman in 1928. Instead of the Rayleigh scattering of photons from the incident light there is also backscattering with wavelength higher than the incident photon. The Raman spectrometer operates with laser as a photon source, because monochromatic and strong beam flux are needed to detect very weak Raman effect. Backscattering is in-elastic and called Stokes Raman, incident photon excites one of the phonons to a virtual energy state, then it returns onto vibrational state which has higher energy than the initial state. Also there is Anti-

Stokes Raman scattering, in this process phonon relaxes back to a lower state in energy after vibrational energy state. Scattering mechanisms and schematic presentation of Raman spectroscopy are shown in Fig.6. Thicknesses of the lines indicate the signal intensity processes between different transitions.

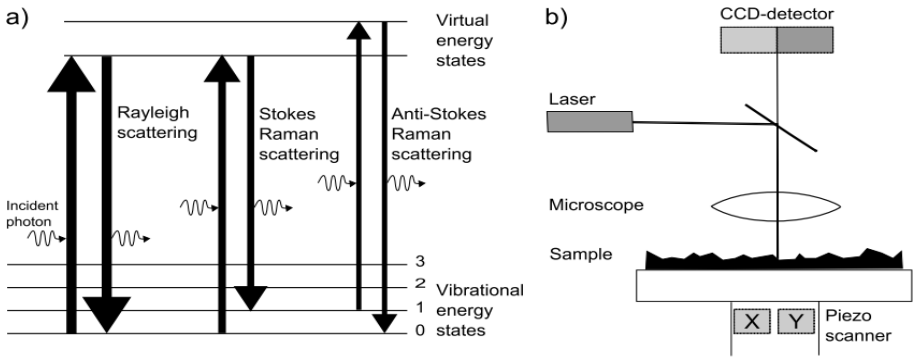

Figure 6. a) Energy level diagram of different types of scattering processes and b) schematic presentation of the Raman spectroscopy [3].

Raman shift is the energy difference between incident photon and the Raman scattered photon and it can be calculated as:

$$\vartheta = \frac{1}{\lambda_i} - \frac{1}{\lambda_s} \qquad (1)$$

Confocal mapping μ-Raman spectroscope includes a 532 nm laser, microscope, detector system and a movable sample stage. Coherent light is guided through optics of microscope to the sample surface, then scattered light is collected and directed to a photodetector. Raman spectrum is acquired by plotting the intensity of the scattered light as a function of the energy difference.

Confocal μ-Raman spectroscopy was used in this thesis to assess the graphene quality. Three main Raman peaks can be used to characterize graphene films (Fig.7). They are D peak at 1345 cm^{-1}, G peak at 1580 cm^{-1} and 2D (G') peak at 2700 cm^{-1}. D peak is related to disorders and vacancies in graphene (defects), G peak is due to in-plane vibration of sp^2 carbon atoms, 2D (G') band reveals information of layer numbers. Monolayer graphene has a sharp and

intense 2D (G') band, with higher intensity than the G peak. Bigger number of layers means broad G' (2D) band and intensity is lower than in case of monolayer while the G peak becomes typically somewhat more intense [26].

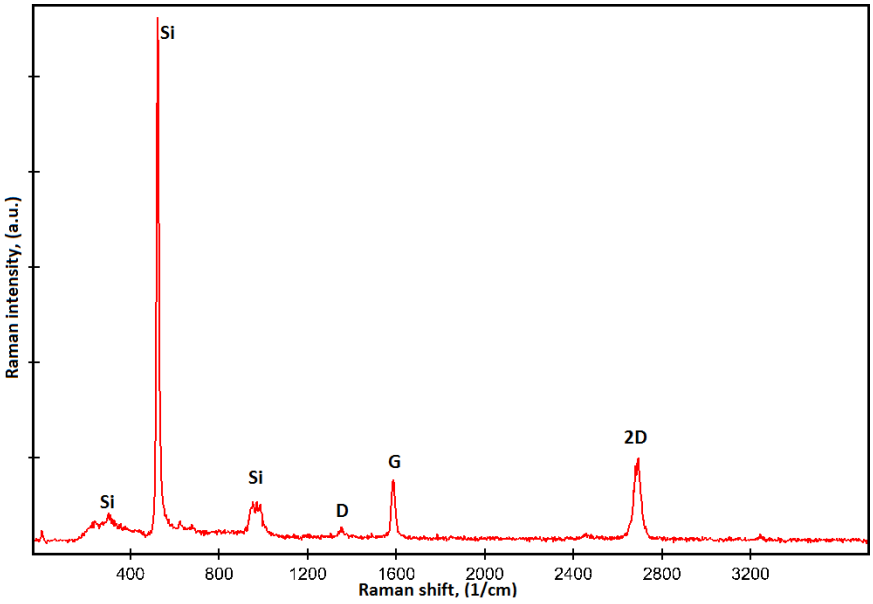

Figure 7. Typical Raman spectrum of a CVD graphene film on a Si/SiO_2 substrate.

3.2 Measuring electrical properties

In this thesis, contact resistance was measured by two methods: transfer length method (TLM) and variation of two- and four-probe methods. TLM gives total resistance between source and drain including both sheet resistance and contact resistance. The four-probe method allows avoiding the parasitic contact resistance and measures directly sheet the resistance only. The contact resistance can be extracted by additional two-probe measurements.

3.2.1 Four-probe method

Four-point probe method is one of the most common methods applied to measure thin film resistivity. In the most common four point probe method, four

probes are at a fixed spacing; current is applied through the outer probes and voltage is measured from the inner probes.

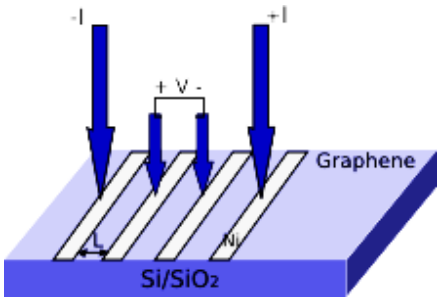

Figure 8. Schematic of the 4-point probe configuration.

Inner probes do not practically carry any current, thus there is no contribution from the parasitic contact resistance (R_c. Combining four-probe measurement with two-probe measurements, allows calculating contact resistance [27]. Hence in the four-point probe setup, the voltage difference between inner probes is given by:

$$V = R_{sheet} I \tag{2}$$

where R_{sheet} is the sheet resistance of graphene, I is the current in the probe. R_{sheet}, in case of equal channel lengths between probes, is given by:

$$R_{sheet} = \frac{W}{L} R_{23} \tag{3}$$

where R_{23} resistance between inner probes.

In the two-point probe setup, instead of R_{sheet} the measurement yields R_{total} which is given by:

$$R_{total} = R_{sheet} \frac{W}{L} + 2R_c \tag{4}$$

where L is channel length and W is channel width. Sheet resistance extracted from four-probe can be used in total resistance, thus we can calculate contact resistance.

3.2.2 Transfer length method

TLM is also widely used measurement technique for thin films (Fig.9). Thin film must have metal contacts, patterned in various distances, at least two different distances; however more contacts will give more reliable result. Various voltages are applied between two contact pads, while the current is measured. Then probes are placed to the next two metal contacts until all have been measured. Assuming that contact resistance is the same for all metal contacts, the change in the total resistance is determined by the graphene resistivity. Sheet resistance is varies depending on a channel length. Total resistance is given by the equation 4.

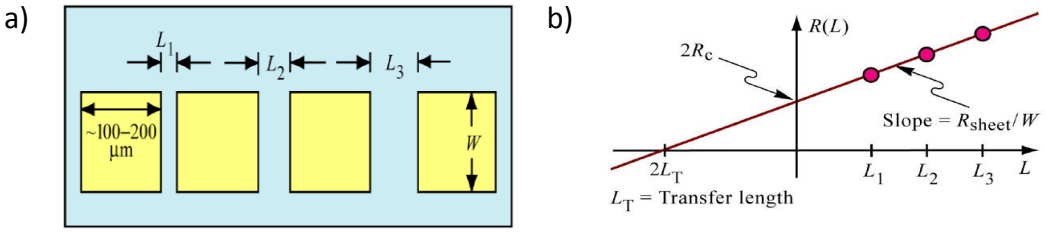

Figure 9. a) Typical schematic of the metal contacts and b) dependence of the total resistance on the channel length [27].

Assuming that the contact resistances are equal, plotting the resistance as a function of channel length will give a straight line. In the limit of a zero-length channel, the residual resistance is twice the value of the contact resistance. Therefore contact resistance can be found from the graph by extrapolating to L=0.

4 Experimental methods

4.1 Graphene transfer

CVD-grown graphene is promising for industrial applications, but samples obtained on metal substrates cannot be used for device fabrication as such. It is necessary to transfer graphene from the copper foil to an insulating substrate. The most commonly used transfer method relies on a Polymethyl-methacrylate (PMMA), which is used as a support layer during the Cu etching. The challenge is in the PMMA residue after removing it in acetone, as it can be a source of carrier scattering, reducing carrier mobility. Also PMMA can reduce adhesion between graphene and contacts increasing the contact resistance. Alternative way to transfer graphene is a "metal method", in which metal is used as an interfacial layer between graphene and PMMA. Both of these methods were used in this work.

Graphene on the copper foil was obtained by CVD method, then sample was covered with uniform thin PMMA layer to support graphene during Cu etching process. To remove graphene from the backside of the copper foil, prior to copper etching, O_2 plasma etching was applied to remove copper effectively. Ammonium persulphate (APS) was used for copper foil etching. Samples were left floating for about 2 hours. When there were no traces of copper, floating graphene was transferred to DI water. Si/SiO_2 substrate was cleaned by RCA method before. After several minutes in DI water, graphene was transferred onto Si/SiO_2 substrate and dried with nitrogen gun. Samples were baked for 300 s at 140 °C in the ambient air to remove moisture for better adhesion of graphene to the substrate and for relaxation of PMMA layer. PMMA was removed in 10 min acetone bath at the room temperature, then it was rinsed in isopropanol for the same time. Process steps are depicted in the Fig.10.

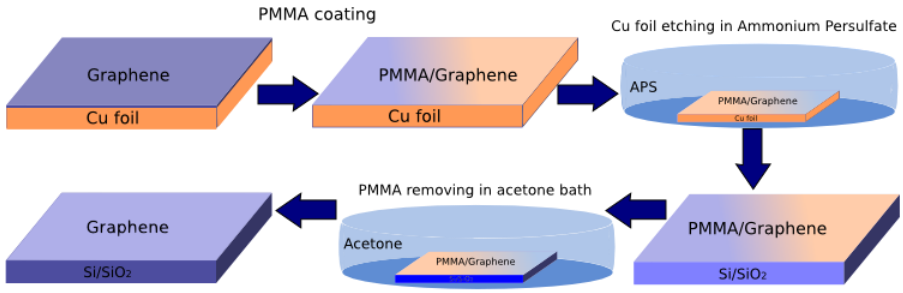

Figure 10. Process steps of the PMMA transfer.

For the alternative transfer method different metals such as Cr, Au and Ni were used as an interfacial layer between graphene and PMMA (Fig.11). Metals were deposited on graphene on the Cu foil with electron beam evaporator. Then, using the same technique as previously, Cu was etched away and graphene with metal on top was transferred on the Si/SiO_2 substrate. The last step of graphene preparation was etching of the metal on top of graphene. After the etching process, the samples were analyzed with Raman spectroscopy.

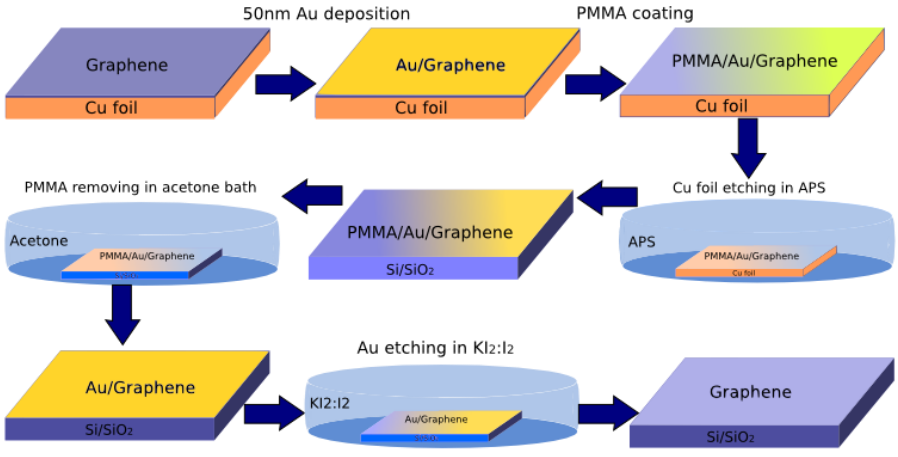

Figure 11. Process steps of the metal assist transfer.

4.2 Device fabrication

On method to reduce contact resistance is based on the efficiency of the edge contacts. Exposed graphene edges at the contact regions were obtained through the catalytic effect of transition metals at high temperature. Schematic of the device fabrication process is shown in the Fig.12. Thin Ni film was deposited at the contact areas. After annealing, large amount of Ni nanoparticles enclosed by zigzag graphene edges formed within the contact regions. Then thick Ni layer was deposited as electrical contacts to the graphene device forming Ni-etched-graphene contacts.

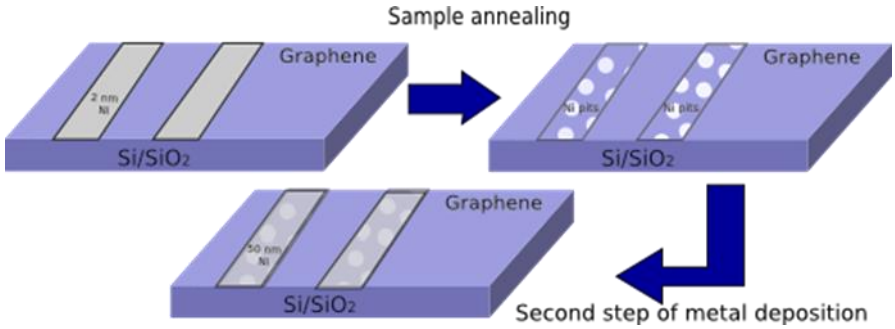

Figure 12. Schematic of the device fabrication.

Electron beam lithography is one of the accurate ways to fabricate semiconductor devices. Graphene devices in this thesis were prepared in four steps using electron beam writer. Layout of the fabricated GFET is shown in the Fig.13. The first step of the fabrication consisted of alignment mark patterning and metal evaporation. Alignment marks were made from gold and are necessary for the alignment in the following steps. In the second step of the lithography, etching areas were patterned to leave only channel area and to improve adhesion between contacts and a substrate. After samples were etched in O_2 plasma. The structure patterning was followed by deposition of thin Ni film and annealing. Last step of the EBL included structures and contact pad patterning to form Ni-etched-graphene contacts. Each of the steps includes

deposition of the positive resist, e-beam exposure, developing, and lift-off process.

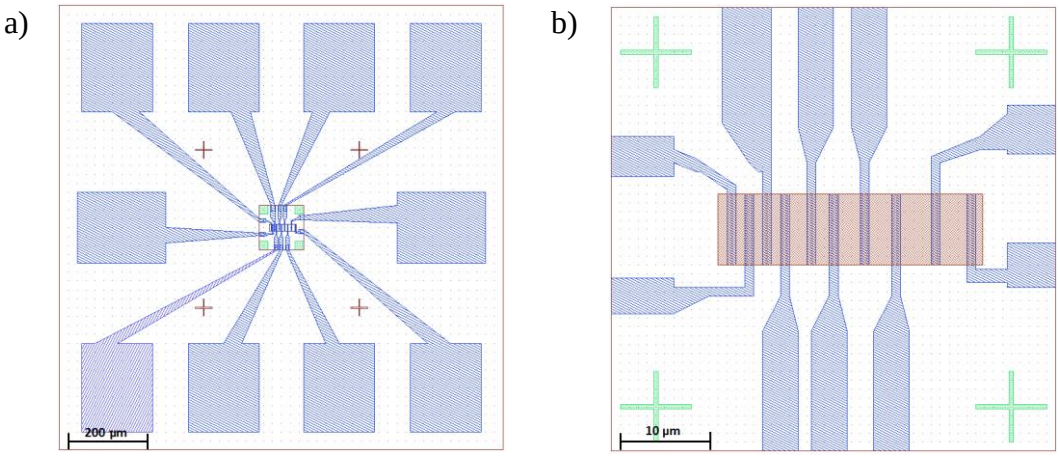

Figure 13. Layout of the GFET a) with contact pads and b) the actual device channel area.

Nickel films were deposited as contacts on the top of graphene after process of electron beam lithography by electron beam evaporator. An electron beam is obtained from a resistively heated filament, the beam is targeted into a crucible containing Ni pellets, thus the metal heats up. As the temperature becomes high enough, metal starts to evaporate. At this point, the sample is placed above the crucible and deposition rate is controlled by the electron beam current. Evaporator tool includes a quartz crystal located next to the sample. Oscillation frequency of the crystal gives information about thickness of the deposited film. Metal evaporation is carried out in a high vacuum, approximately 10^{-6}-10^{-7} mbar.

Annealing of the samples was carried out at 580 °C in the presence of argon and hydrogen gas mixture at a pressure 12 Torr with rapid thermal process (RTP). Infrared lamps provide rapid heating of the chamber. They are arranged in three zones with separate power controls. Temperature was controlled by power and monitored by thermocouple. Si wafer was used as a susceptor.

Etchings of graphene from the backside of the copper foil and during EBL process were carried out in ICP-RIE tool. During this process O_2 plasma is

produced, thus in the presence of argon and applied forward bias, graphene etching takes place.

5 Results and discussion

5.1 Quality of the graphene sheets

The first step of this work was to transfer graphene from the copper foil to a target substrate Si/SiO_2. Transferred samples were analyzed using optical microscopy, confocal μ-Raman spectroscopy and finally with SEM. Raman spectrum of the graphene sheet used for device fabrication is shown in Fig.7. Histograms show that 2D peak is more intense than G peak (Fig.14b) and D/G ratio is almost zero (Fig.14a), which means that we have high quality monolayer graphene with very small number of defects.

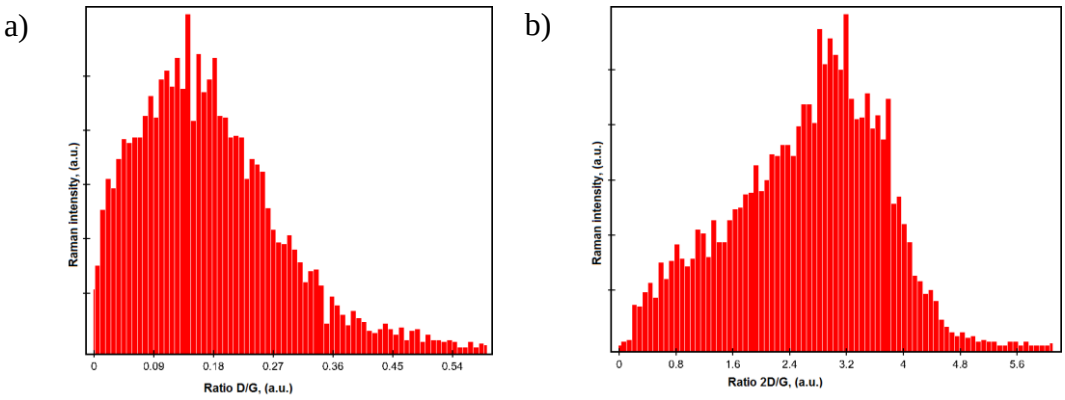

Figure 14. a) Histogram of the D/G ratio and b) histogram of the 2D/G ratio. (Mapping area of $10^{*}10$ μm^2)

We obtained uniform graphene films without folds and ruptures; the color contrast indicates that the film has some bilayer areas. Fig.15 shows SEM images of transferred graphene sheets (electron acceleration voltage was ~5 kV). The difference in contrast makes it possible to identify bilayer graphene areas: dark areas in the form of flakes mean bilayer and dark stripes are wrinkles.

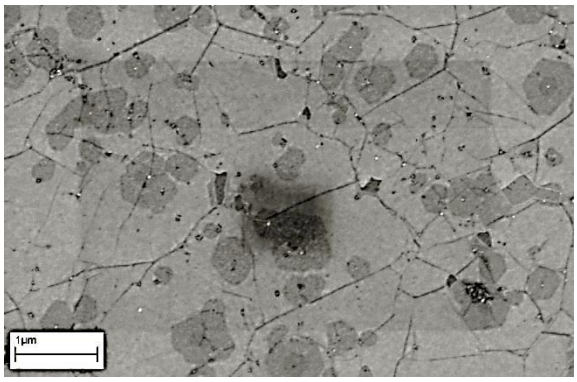

Figure 15. SEM image of graphene after transfer.

5.1.1 Comparison of PMMA and metal transfer

Prior to the actual study of contact resistance, different transfer method were examined. In the typical transfer method, PMMA used for graphene transfer cannot be perfectly removed, which deteriorates the contact performance of graphene devices. Even after several cleaning processes such as vacuum annealing or ozone treatment some polymer residue can still remain on the graphene [28]. A “metal-assisted” transfer method avoids contact between the polymer and graphene. Moreover, metal film used in transfer can be directly used to form contacts in device fabrication. It can considerably reduce the time and optimize the processing device fabrication. In this study chromium, gold, nickel and palladium were used as interfacial layers. Quality of graphene after metal etching was examined using confocal µ-Raman spectroscopy. After transfer samples with Ni and Pd as assisting layers did not show main graphene peaks in Raman, indicating that there is no graphene layer. Raman spectra of transferred graphene using Cr and Au as interfacial layer are compared with the PMMA method are plotted in the Fig.16.

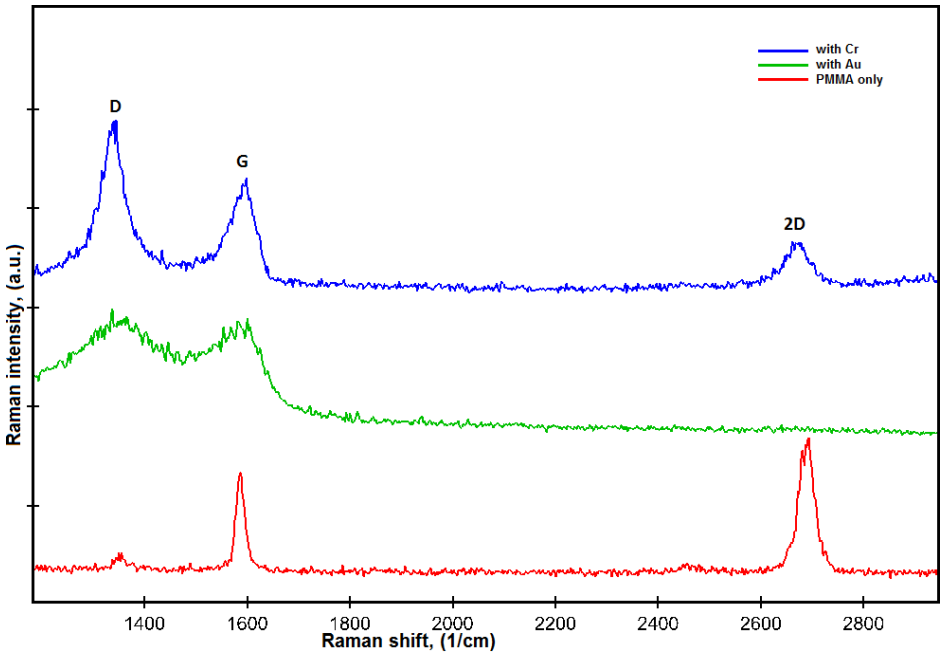

Figure 16. Raman spectra of the samples obtained by PMMA and metal transfer methods.

The Raman spectrum of Cr assist transfer exhibit G band, 2D band shifted to ~2650 cm^{-1} and D band centered at ~1320 cm^{-1}. An increase of the D peak intensity confirms the presence of defects, which were possibly induced during the metal etching. In case of Au assisted transfer, there is no 2D peak at all. However, D and G bands indicate that we have carbon or graphitic material on the surface. Fig.17 shows SEM images of the samples surface after metal transfer. Transfer with Cr in the Fig.17a shows large number of voids and ruptures. This can explain high D band in the Raman spectrum. In the Fig.17b dark dots are related to the carbon residue. Although the metal assisted method seems promising, further process development is required.

a) 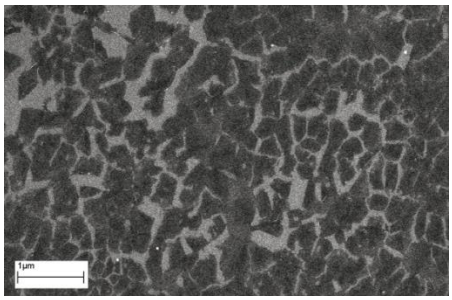 b) 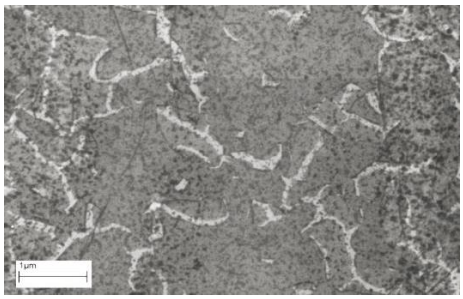

Figure 17. SEM image of samples surface after the metal transfer a) with Cr and b) with gold.

5.2 Electron beam lithography

Due to the fact that the metal transfer requires optimization of the process to achieve comparable quality of graphene layers with films obtained by PMMA method, it was decided to use graphene layers transferred with PMMA only. In the EBL process, methyl-methacrylate (MMA) was used as copolymer resist with PMMA, 1000 Å of MMA and 1500 Å of PMMA were spin coated and baked for 120 s on a hot plate. Developer used was diluted MIBK with IPA (1:1). Lift-off process was done using acetone and IPA. Thickness of evaporated gold used for alignments marks was 50 nm. To have device suitable for both electrical measurement methods the channel lengths of graphene was varied using 2 µm, 3 µm, 5 µm and 7 µm (Fig.13) channel lengths. Thickness of Ni used for creating graphene edges was 2 nm, and for contacts it was 50 nm.

a) 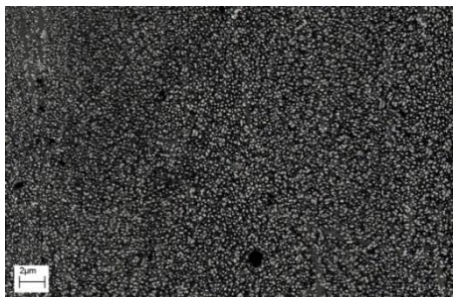 b) 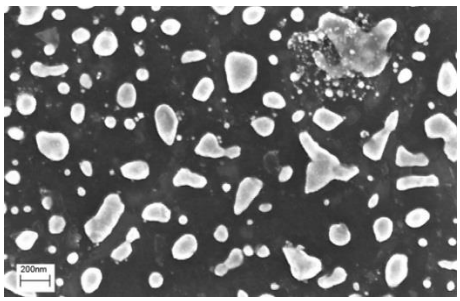

Figure 18. SEM image of the contact area after annealing.

During the annealing Ni nanoparticles were formed. Fig.18 shows an SEM image of the Ni nanoparticles. The size of the Ni islands depends on thickness of the Ni film. In reference [19], the authors estimated that the size of the Ni islands

changes from 7 to 27 nm, with an average of 12 nm, in case of 2-nm-thick Ni layer. Resolution of SEM used in this work does not allow, to estimating the size of the Ni islands for 2 nm thick layer. However, in case of 10-nm-thick layer average size of the islands is ~80 nm and their areal density is lower than with 2 nm thick layer.

5.2.1 Annealing parameters

Critical part of the fabrication process was to preserve the high quality of graphene in the channel area during the annealing. The presence of hydrogen is very important in forming of the Ni islands. On the one hand, hydrogen and pressure affects on the surface tension and the melting temperature. On the other hand, H_2 attacks graphene imperfections and creates defects. Forming of metal islands on the graphene surface is related to melting of the metal, but as it is known that at too high temperature, transition metals start moving and etch the surface at the same time [22]. To prevent this movement H_2 presence is necessary. In reference [29], it is reported that defects to graphene caused by hydrogen would originate from a high partial pressure.

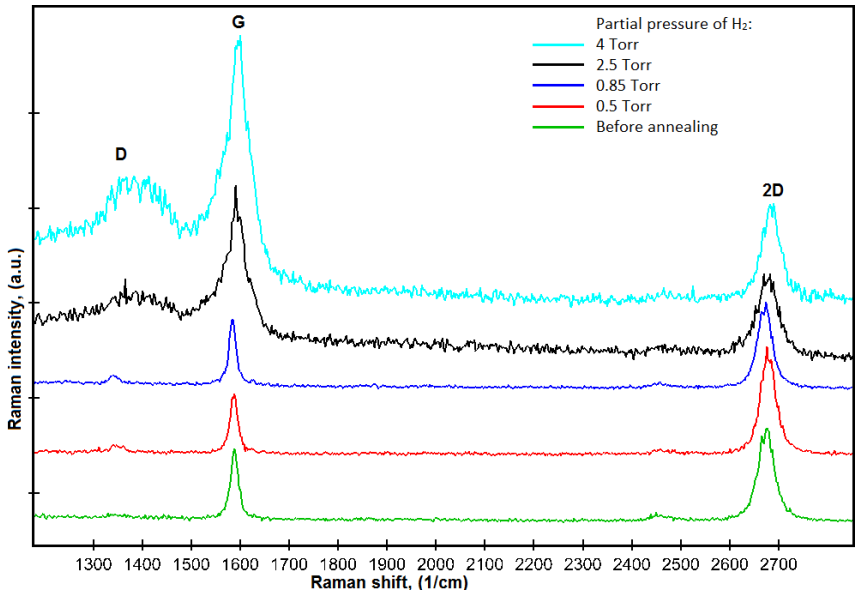

Figure 19. Raman spectra of the samples annealed with various partial pressure of H_2.

In the Fig.19 are shown the Raman spectra of the channel area after the annealing process with various partial pressure of H_2. By optimizing the temperature and gas flow parameters it was possible to obtain Ni metal islands while preserving graphene quality.

Table 1. Hydrogen flow, partial preassure and total preassure used for the annealing test.

H_2 flow, (sccm)	Partial H_2 preassure, (Torr)	Total pressure, (Torr)
70	4	12
35	2.5	12
10	0.85	12
5	0.5	12

Temperature during the optimized annealing process were kept at about 580 °C at a pressure of 12 Torr with total gas flow of 135 sccm of Ar:H_2 mixture (100:4). Time of the annealing treatment was 10 min. It can be noticed in the Fig.19 can be noticed that the spectrum shows insignificant D band and slightly decreased 2D/G ratio in case of the H_2 gas flow of 5 sccm. This indicates the preservation of the graphene quality.

5.3 Electrical measurements

Electrical measurements were carried out under ambient conditions. TLM data measured is plotted in the Fig.20. The random distribution of the total resistance means that this data is not reliable for extracting contact resistance. Sheet resistance measured with four-point probe method was ~2000 Ω/□.

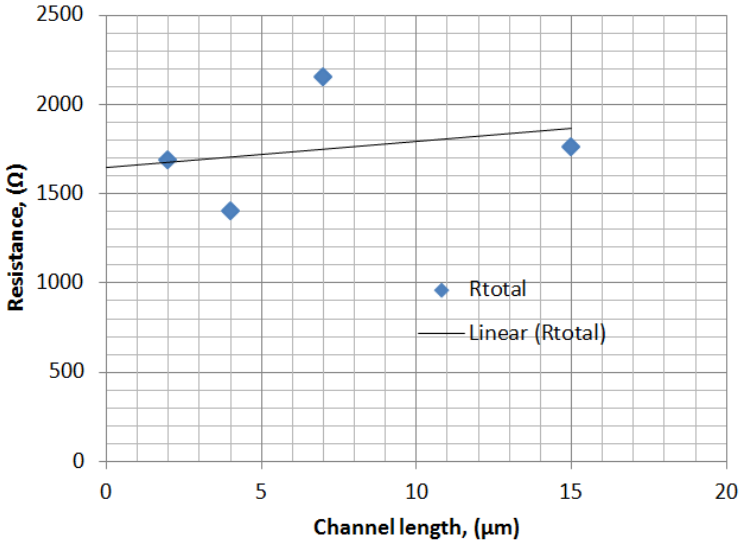

Figure 20. TLM data for the Ni etched samples.

This non-linear change of total resistance versus the channel length may be a consequence of the contacts moving during the lift-off process. As it was mentioned previously, the adhesion between Ni and graphene is weak and it is further reduced with reducing Ni thickness. In the process shown in the Fig.12, 2 nm thick Ni contacts could have been displaced during the lift-off process. Thus, in the last lithography step contact pads and structures can be not exactly over the previous structure. Channel width in this case cannot be assumed as in designed layout of the structure.

5.4 Reference sample

Reference sample was fabricated to compare contact resistance. The quality of this sample was investigated using the same techniques and it was found similar to be. It had the same kind of the Raman spectrum, and good uniformity in the SEM images. Device fabrication was the same, excluding steps with deposition of 2 nm thick Ni layer and the annealing. Electrical measurements applied for this sample was also the same. TLM data of the reference sample is displayed in the Fig.21.

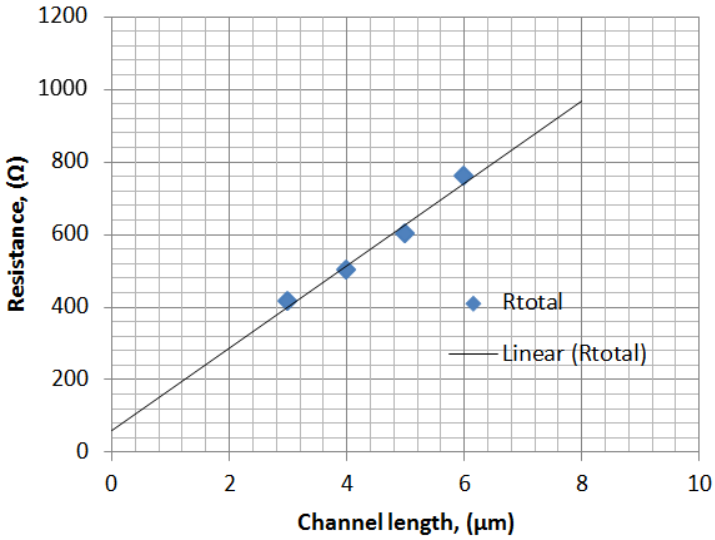

Figure 21. TLM data of the reference sample.

Calculated contact resistance for the reference sample was found at ~350 Ωµm, extracted sheet resistance equal to 1100 Ω/□. The result of the sheet resistance was also confirmed by the 4-probe method. These values are reasonably good compared to values reported in the literature. Contact resistance for such metals as Cr, Pd and Ti/Au vary between 100 Ωµm and 800 Ωµm [28] [19] [18].

6 Summary

In this thesis, ways to reduce contact resistance were studied. The work included investigation of transferred CVD graphene films by different techniques, fabrication of electronic device using EBL and measuring of the contact resistance by TLM and four-probe methods. Graphene was mainly characterized by optical microscopy, confocal scanning μ-Raman spectroscopy and scanning electron microscopy.

The first part of the experiments consisted of device fabrication process optimization. Here the focus was on the "metal-assisted" transfer method, where metal is applied as an interfacial layer to avoid direct contact of PMMA with graphene. Minimizing PMMA residue is expected to reduce contact resistance. However, transferred graphene films obtained using this method showed somewhat lower quality than the PMMA assisted method. The method of using metal between graphene and PMMA requires further process optimization. Among the metals tested (Ni, Pd, Au, Cr), the best results were achieved using Cr.

Maximizing edge-contacted current injection between graphene and metal was used to reduce contact resistance. After deposition of a Ni thin film on the top of graphene, samples were annealed to form Ni nanoparticles and to catalytically etch graphene near Ni nanoparticles. Critical part of the fabrication process was to preserve the high quality of the graphene in the device channel area during the annealing. The presence of hydrogen is very important in forming of the Ni islands, but it can also create defects in graphene. Obtaining Ni islands and preserving of graphene quality were achieved by optimizing the temperature and gas flows. Obtained distribution of total resistance depended on channel length of the annealed sample was not reliable to extract contact resistance. This can be related to low adhesion between Ni and graphene, which relates to processing difficulties and to possible damage induced to the graphene channel during annealing process. In the final stage the reference sample

without annealing process was analyzed. It showed a rather low value of contact resistance ~350 Ωμm; this is comparable with the latest reported values.

This work serves as a basis for several further investigations. The investigation of the reducing contact resistance could be continued by optimizing the process regardless the difficulties related to the low adhesion of Ni on graphene. Also further study of device fabrication by applying “metal-assisted” transfer can play an important role in reducing the contact resistance. Conventional Ni contacts have already given good results for contact resistance in this work; therefore applying additional contact treatments can be expected to give improved results.

References

[1] K. S. Novoselov A. K. et al. Geim, "The rise of graphene", *Nature Materials*, pp. 183-191, June 2007.

[2] K. S. Novoselov, "Electric field effect in atomically thin carbon films", *Science*, vol. 306, no. 5696, pp. 666-669, 2004.

[3] V. Singh and D. Joung, "Graphene based materials: Past, present and future", *Science*, vol. 56, no. 8, pp. 1178-1271, 2011.

[4] Z. Song, T. Li, X. Li, A. Ogbazghi, R. Feng, C. Berger, "Ultrathin epitaxial graphite: 2D electron gas properties and a route toward graphene-based nanoelectronics", *Physic Chemistry*, vol. 108, no. 52, pp. 19912-6, 2004.

[5] H. Kim, Y. Lee, X. Xu, J-S. Park, Y. Zheng, "Roll-to-roll production of 30-inch graphene films for transparent electrodes", *Nature Nanotechnoly*, vol. 5, pp. 574-578, June 2010.

[6] A. Bostwick, K. Horn, J. Jobst, G. L. Kellogg, L. Ley, K. V. Emtsev, "Towards wafer-size graphene layers by atmospheric pressure graphitization of silicon carbide", *Nature Material*, vol. 8, no. 3, pp. 203-207, 2009.

[7] A. Presland. and P. Walker, "Growth of single-crystal graphite by pyrolysis of acetylene over metals", *Carbon*, vol. 7, pp. 1-8, October 1969.

[8] A. Reina and J. Kong, "Graphene Growth by CVD Methods", *Graphene Nanoelectronics*, Springer, 2012, ch. 7, pp. 167-203.

[9] M. Losurdo, M. Giangregorio, P. Capezzuto, and G Bruno, "Graphene CVD growth on copper and nickel: role of hydrogen in kinetics", *Physical Chemistry Chemical Physics*, vol. 13, no. 46, pp. 20836-20843, September 2011.

[10] J. Riikonen et al., "Photo-thermal chemical vapor deposition of graphene on copper", *Carbon*, vol. 62, pp. 43-50, 2013.

[11] F. Schwierz, "Graphene transistors", *Nature nanotechnology*, vol. 5, no. 7, pp. 487-496, 2010.

[12] W. Yuan and G. Shi, "Graphene-based gas sensors", *Journal of Materials Chemistry*, vol. 1, no. 35, p. 10078, 2013.

[13] Z. Gu, H. Pan, M. Wu, Y. Li, and Y. Chen, "Graphene-based functional materials for organic solar cells", *Optical Materials Express*, vol. 2, no. 6, pp. 814-824, 2012.

[14] T.V. Blank and Yu.A. Goldberg, "The current flow mechanism in metal-semiconductor ohmic contacts", *Phyzika i Technika Poluprovodnikov*, vol. 41, no. 11, pp. 1281-1308, 2007.

[15] S. Song, J. Park, O. Sul, and B. Cho, "Determination of work function of graphene under a metal electrode and its role in contact resistance", *Nano letters*, vol. 12, no. 8, pp. 3887-3892, 2012.

[16] K. Nagashio, T. Nishimura, K. Kita, and A. Toriumi, "Contact resistivity and current flow path at metal/graphene contact", *Applied Physics Letters*, vol. 97, no. 14, p. 143514, 2010.

[17] Y. Khatami and H. Li, "Metal-to-Multilayer-Graphene Contact — Part I : Contact Resistance Modeling", *IEEE*, vol. 59, no. 9, pp. 2444-2452, 2012.

[18] J. T. Smith, A. D. Franklin, D. B. Farmer, and C. D. Dimitrakopoulos, "Reducing contact resistance in graphene devices through contact area patterning", *ACS nano*, vol. 7, no. 4, pp. 3661-7, 2013.

[19] W. Leong, H. Gong, and J. Thong, "Low-Contact-Resistance Graphene", *ACS nano*, no. 1, pp. 994-1001, 2014.

[20] R. Sahin, E. Simsek, and S. Akturk, "Nanoscale patterning of graphene through femtosecond laser ablation", *Applied Physics Letters*, vol. 104, no. 5, p. 053118, 2014.

[21] M. Lukas et al., "Catalytic subsurface etching of nanoscale channels in graphite", *Nature communications*, vol. 4, p. 1379, 2013.

[22] V. Manfrinato, R. Leonardo, C. Campos, J. Sanchez-Yamagishi, J. Kong, and P. Jarillo-Herrero, "Anisotropic Etching and Nanoribbon Formation in Single-Layer Graphene", *Nano letters*, vol. 9, no. 7, pp. 2600-4, 2009.

[23] P. Hill, E. W. Blake et al., "Making graphene visible", *Applied Physics Letters*, vol. 91, no. 6, 2007.

[24] L. Gao, W. Ren, F. Li, and H. Cheng, "Total color difference for rapid and accurate identification of graphene", *ACS Nano*, vol. 2, no. 8, 2002.

[25] M. Her, R. Beams, and L. Novotny, "Graphene transfer with reduced residue", *Physics Letters A*, vol. 377, no. 21-22, pp. 1455-1458, 2013.

[26] A. C. Ferrari et al., "Raman spectrum of graphene and graphene layers", *Physical Review Letters*, vol. 97, no. 18, 2006.

[27] M. B. Klarskov et al., "Fast and direct measurements of the electrical properties of graphene using micro four-point probes", *Nanotechnology*, vol. 22, pp. 445702-445708, 2011.

[28] J. Lee et al., "Clean transfer of graphene and its effect on contact resistance", *Applied Physics Letters*, vol. 103, no. 10, p. 103104, 2013.

[29] C. Kang, M. Kim, H. Cheong, H. Lee, and J. S. Lee, "Effects of Hydrogen Partial Pressure in the Annealing Process on Graphene Growth", *Physical Chemistry*, vol. 118, pp. 3574-3580, 2014.

[30] Y. P. Chen, D. D. Nolte, X. Wang, "Strong Anomalous Optical Dispersion of Graphene: Complex Refractive Index Measured by Picometrology", *Optics Express*, vol. 16, no. 26, pp. 22105-22112, 2008.